Journal of Manufacturing Engineering, 2008, Vol.3, Issue.1

MICROMECHANICAL ANALYSIS OF FRP HYBRID COMPOSITE LAMINA FOR OUT-OF-PLANE TRANSVERSE LOADING

K Sivaji Babu[1], Dr. K Mohana Rao[2], Dr. V Ramachandra Raju[3], Dr. V Bala Krishna Murthy[4], & MSR Niranjan Kumar[5].

[1] Lecturer, Mechanical Engg. Department, V.R. Siddhartha Engineering College, Vijayawada, A.P, India.
[2] Principal, Sir C. R. Reddy College of Engineering, Eluru, A.P., India.
[3] Principal , J.N.T. University, Vizayanagaram, A.P., India.
[4] Professor, Mech. Engg. Dept., P. V. P. Siddhartha Institute of Technology, Vijayawada – 520 007, A.P, India.
[5] Sr. Lecturer, Production Engg. Department, V.R. Siddhartha Engineering College, Vijayawada, A.P, India.

ABSTRACT

The present investigation studies the micromechanical behavior of the square unit cell of a hybrid fiber reinforced composite lamina. A three-dimensional finite element model has been developed from the unit cells of square pattern of the composite to predict the Young's modulus (E_3) and poisson's ratios (ν_{31} and ν_{32}) of Graphite-Boron hybrid fiber reinforced lamina for various volume fractions. The stresses at the fiber-matrix interfaces are also determined from these models. The finite element software ANSYS has been successfully executed to evaluate the properties and stresses. The variation of the stresses at the fiber-matrix interface with respect to the angular location is discussed.

Key Words: FRP, FEM, Micromechanics, Hybrid Lamina

1. INTRODUCTION

1.1 ELASTIC PROPERTIES

Fiber reinforced composites can be tailor made, as their properties can be controlled by the appropriate selection of the substrata parameters such as fiber orientation, volume fraction, fiber spacing, and layer sequence. The required directional properties can be achieved in the case of fiber reinforced composites by properly selecting various parameters enlisted above. As a result of this, the designer can have a tailor-made material with the desired properties. Such a material design reduces the weight and improves the performance of the composite. For example, the carbon-carbon composites are strong in the direction of the fiber reinforcement but weak in the other directions. Elastic constants of fiber reinforced composites with various types of constituents were determined by Chen and Chang [1] Hashin and Rosen [2], Hashin [3] and Whitney [4].

It is clear from the above predictions that four of the five independent composite modulii (E_1, E_2, ν_{12}, G_{12} and G_{23}) differ only in their expressions for the fifth elastic constant i.e., transverse shear modulus, which varies between two bounds that are reasonably close for the cases of practical interest. The values of elastic modulii presented by Hashin and Rosen [2] have very close bounds. Ishikawa *et al* [5] experimentally obtained all the independent elastic modulii of unidirectional carbon-epoxy composites with the tensile and torsional tests of co-axis and off-axis specimens. They confirmed the transverse isotropy nature of the graphite-epoxy composites. Hashin [6] comprehensively reviewed the analysis of composite materials with respect to mechanical and materials point of view. Expressions for E_1 and G_{12} are derived using the theory of elasticity approach [7].

1.2 MICROMECHANICS

Micromechanics is intended to study the distribution of stresses and strains within the micro regions of the composite under loading. This study will be particularized to simple loading and geometry for evaluating the average or global stiff nesses and strengths of the composites[8]. Micromechanics analysis can be carried theoretically using the principles of continuum mechanics, and experimentally using mechanical, photo elasticity, ultrasonic tests, etc. The results of micromechanics will help

- to understand load sharing among the constituents of the composites, microscopic

Corresponding author: *k_sivajibabu@rediffmail.com*

structure (arrangement of fibers), etc., within composites,

- to understand the influence of microstructure on the properties of composite,
- to predict the average properties of the lamina, and
- to design the materials, i.e., constituents volume fractions, their distribution and orientation, for a given situation.

The properties and behavior of a composite are influenced by the properties of fiber and matrix, interfacial bond and by its microstructure. Micro structural parameters that influence the composite behavior are fiber diameter, length, volume fraction, packing and orientation of fiber. A closed form micromechanical equation for predicting the transverse modulus, E_2, of continuous fiber reinforced polymers is presented[9].

Anifantis[10] predicted the micromechanical stress state developed within fibrous composites that contain a heterogeneous inter phase region by applying finite element method to square and hexagonal arrays of fibers. Sun *et al* [11] established a vigorous mechanics foundation for using a Representative Volume Element (RVE) to predict the mechanical properties of unidirectional fiber composites. Li[12] has developed two typical idealized packing systems, which have been employed for unidirectional fiber reinforced composites, viz. square and hexagonal ones to accommodate fibers of irregular cross sections and imperfections asymmetrically distributed around fibers. To understand the mechanism of the 'hybrid effect' on the tensile properties of hybrid composites Yiping Qiu & Peter Schwartz[13] investigated the fiber/matrix interface properties by using single fiber pull out from a micro composite (SFPOM) test, which showed a significant difference between the interfacial shear strength of Kevlar fiber/epoxy in single fiber type and that in the hybrid at a constant fiber volume fraction, which shortened the ineffective length and contributed to the failure strain increase of Kevlar fibers in the hybrid. Mishra & Mohanthy et al[14] investigated the degree of mechanical reinforcement that could be obtained by the introduction of glass fibers in bio fiber (pineapple leaf fiber/ sisal fiber) reinforced polyester composite experimentally. Addition of relatively small amount of glass fiber to the pineapple leaf fiber and sisal fiber reinforced polyester matrix enhanced the mechanical properties of the resulting hybrid composites. The works reported in the available literature do not include the micromechanical analysis of hybrid FRP lamina using FEM. The present work aims do develop a 3-D finite element model for the micromechanical analysis of hybrid composite lamina.

1.3 SQUARE ARRAY OF UNIT CELLS

A schematic diagram of the unidirectional fiber composite is shown in **Fig.1** where the fibers are arranged in the square array. It is assumed that the fiber and matrix materials are linearly elastic. A unit cell is adopted for the analysis. The cross sectional area of the fiber relative to the total cross sectional area of the unit cell is a measure of the volume of fiber relative to the total volume of the composite. This fraction is an important parameter in composite materials and is called fiber volume fraction (V_f).

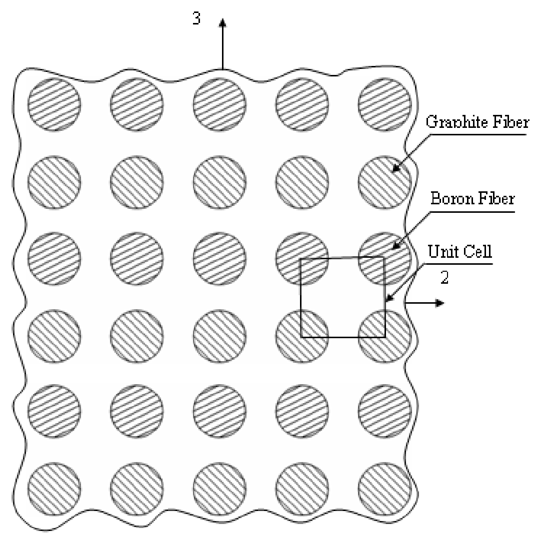

Fig.1 Concept of Unit Cells

2. PROBLEM STATEMENT

The analysis deals with the evaluation of the out-of-plane Transverse Young's Modulus E_3, Poison's Ratios ν_{31}, ν_{32} and determination of the stresses at the fiber-matrix interfaces for a complete possible range of fiber volume fractions using 3-D finite element method developed based on theory of elasticity.

2.1 Finite Element Model

The 1-2-3 Coordinate system shown in **Fig.2** is used to study the behavior of unit cell. The isolated unit cell behaves as a part of large array of unit cells by satisfying the conditions that the boundaries of the isolated unit cell remain plane.

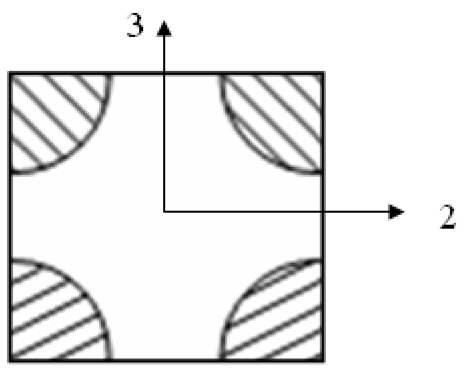

Fig. 2 Isolated Unit Cell of Square packed array

It is assumed that the geometry, material and loading of unit cell are symmetric with respect to 1-3 plane. Therefore, a one-fourth portion of the unit cell is modeled for the analysis (Fig. 3).

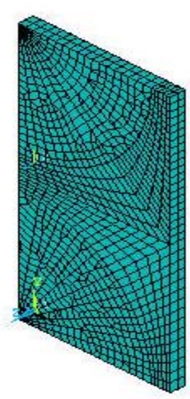

Fig. 3 Finite Element mesh on one-fourth Portion of the unit cell

2.2 Geometry

The dimensions of the finite element model are taken as

- X=100 units (in-plane Transverse direction)
- Y=200units(out-of-planeTransverse direction)
- Z=10 units (Fiber direction).

The radius of fiber is varied corresponding to the volume fraction. For example, the radius of the fiber is calculated as 61.8 units, so that the fiber volume fraction becomes 0.30.

2.3 Element Type

The element used for the present analysis is SOLID 95 of ANSYS software [15] which is developed based on three-dimensional elasticity theory and is defined by 20 nodes having three degrees of freedom at each node: translation in the node x, y and z directions.

2.4 Materials

The properties of the constituent materials used for the present analysis are given in Table1.

Table1. Properties of Constituents [7]

S. No.	Material	E (GPa)	ν	G (GPa)
1	Graphite Fiber	233 - axial 23.1 - radial	0.2 (long. Plane) 0.4 (Tran. Plane)	8.96 (long. Plane) 8.27 (Tran. Plane)
2	Boron Fiber	400	0.2	--
3	Epoxy Matrix	4.62	0.36	--

2.5 Loading

Uniform tensile load of 1 MPa is applied on the area at Y = 200 units.

2.6 Boundary conditions

Due to the symmetry of the problem, the following symmetric boundary conditions are used

- At x = 0, $U_x = 0$
- At y = 0, $U_y = 0$
- At z = 0, $U_z = 0$

In addition the following multi point constraints are used.

- The U_x of all the nodes on the line at x =100 is same
- The U_y of all the nodes on the line at y =200 is same
- The U_z of all the nodes on the line at z = 10 is same

3. RESULTS

The mechanical properties of the laminae are calculated using the following expressions. Young's modulus in out-of-plane transverse direction

$$E_3 = \frac{\sigma_3}{\varepsilon_3} \qquad \text{Poisson's Ratios } \nu_{31} = \frac{-\varepsilon_1}{\varepsilon_3};$$

$$\nu_{32} = \frac{-\varepsilon_2}{\varepsilon_3}$$

Where σ_3 = Stress in 3-direction (Y)

ε_1 = Strain in 1-direction (Z)
ε_2 = Strain in 2-direction (X)
ε_3 = Strain in 3 –direction(Y)

Sufficient numbers of convergence tests are made and the present finite element model is validated by comparing the Young's modulus of FP-Al lamina predicted with the value from the available literature [16] and found close agreement (Fig. 4).

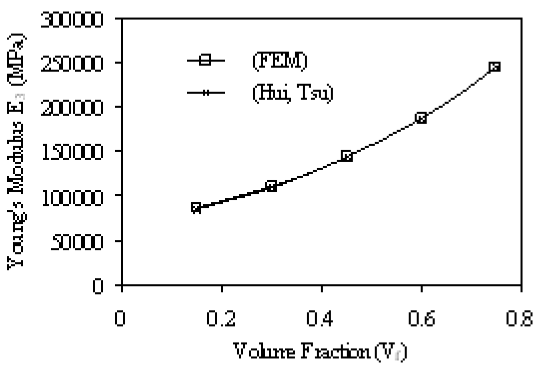

Fig. 4 Variation of Young's Modulus (E_3) With respect to volume fraction

Fig 5 presents the mechanical properties predicted from the present analysis. Later the finite element models are used to evaluate the properties E_3, ν_{31}, ν_{32} and the stresses at the fiber matrix interface of a hybrid composite with boron and graphite fibers.

4. Analysis of Results

4.1 Variation of Young's Modulus (E_3) With Respect To Volume Fraction:

It is observed that there is a linear increment of the young's modulus with respect to volume fraction for all the three combinations up to V_f = 45%. For V_f from 45% to 60% the young's modulus increases at a slow rate. For V_f between 60% and 75% it increases at faster rate for Boron-epoxy and Hybrid-epoxy composites. This is because the stiffness of the composite increases with increase in V_f. The young's modulus of Boron-epoxy at all the volume fractions is observed to be maximum followed by hybrid-epoxy and Graphite-epoxy, due to the less value of graphite fiber transverse modulus when compared with boron fiber modulus. (Fig.5)

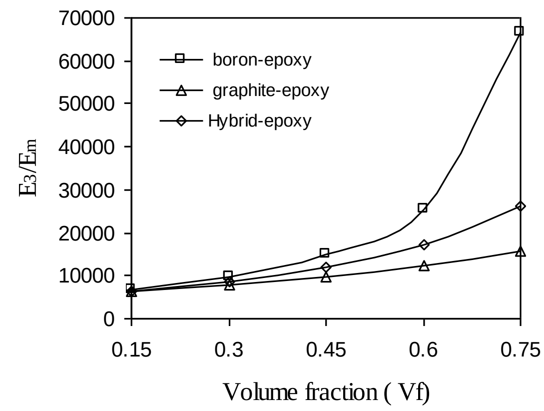

Fig. 5 Variation of Young's Modulus (E_3) with respect to volume fraction

4.2 Variation 0f Poisson's Ratio (ν_{31} and ν_{32}) With Respect To Volume Fraction:

The Poisson's Ratios (ν_{31}) decreases from V_f =15% to 45%, and later increases for Boron-epoxy and hybrid-epoxy. For Graphite-epoxy it shows a decreasing trend throughout. (Fig.6)

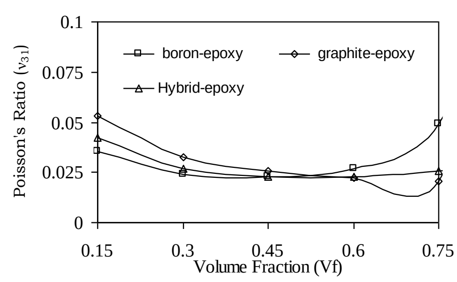

Fig. 6 Variation of Poisson's Ratio (ν_{31}) with respect to volume fraction

The Poisson's Ratios (ν_{32}) gradually decreases with the increase in volume fraction for all the three combinations. (Figs.7). The rate of decrease is more for Boron-epoxy followed by hybrid-epoxy.

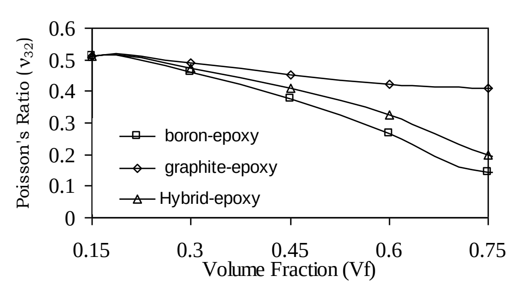

Fig. 7 Variation of Poisson's Ratio (ν_{32}) with respect to volume fraction

The following stresses are computed at the fiber-matrix interface.

- σ^f_n = Normal stress in the fiber at the interface
- σ^m_n = Normal stress in the matrix at the interface
- τ^f_{ns} = Shear stress in the fiber at the interface.
- τ^m_{ns} = Shear stress in the matrix at the interface.
- σ^f_c = Circumferential stress in the fiber at the interface
- σ^m_c = Circumferential stress in the matrix at the interface

4.2.1 Stresses at bottom interface

The results are normalized with the applied pressure. Fig. 8 shows the variation of interface normal stress in fiber and matrix with respect to θ, where θ is the angle measured from direction 2 in the counter-clockwise sense. The normal stress is observed to be compressive for V_f =15% and 30% up to θ = 18^0 and is tensile between θ = 18^0 and θ = 90^0 . For V_f =60% and 75% the normal stress is tensile for all the values of θ. The magnitude of the stress is observed to be maximum at θ = 90^0 for all volume fractions. It is observed that the maximum stress decreases with increase in V_f.

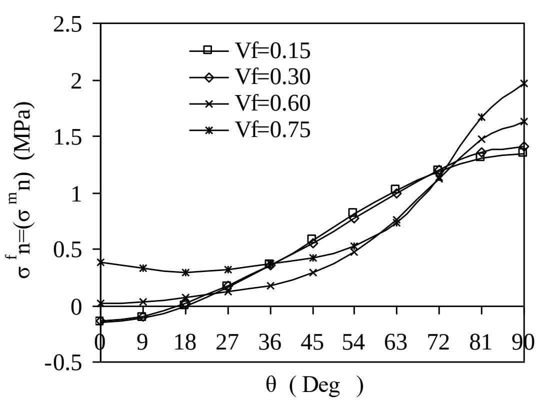

Fig. 8 Variation of bottom interface Normal stress with respect to θ

The variation of the interface shear stress in the constituent materials with respect to θ is shown in Fig.9. The magnitude of the shear stress is observed to be maximum at θ = 45^0 for volume fractions of 15% and 30%. For V_f =60% and 75% stress is maximum at θ = 63^0 and 72^0 respectively. It is also observed that the magnitude of maximum shear stress decreases with increase in V_f.

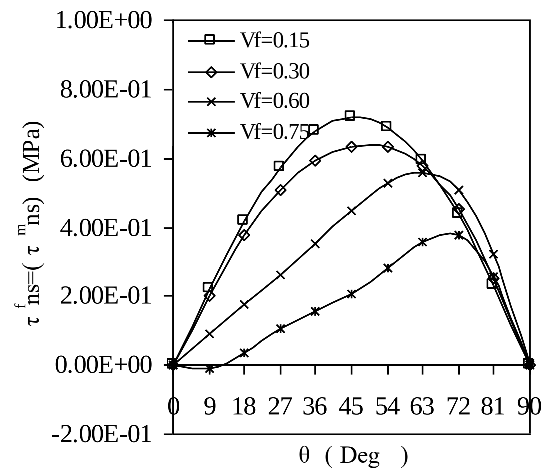

Fig. 9 Variation of bottom interface Shear stress with respect to θ

Fig. 10 shows the variation of interface circumferential stress in the fiber material with respect to θ. The stresses are observed to be tensile for V_f = 60% and 75%. For V_f = 15% the stress is observed to be tensile up to θ = 72^0 and is compressive in between72^0 and 90^0. For V_f = 30% the stress is observed to be tensile up to θ = 81^0 and is compressive in between 81^0 and 90^0. The magnitude of the circumferential stress is observed to be maximum at θ = 0^0 for V_f =15%, 30% .For V_f = 60% and 75% it is maximum at θ = 18^0 and θ = 90^0 respectively .The magnitude of the maximum circumferential stress decreases with increase in V_f at θ = 0^0 and increases with increase in V_f at θ = 90^0.

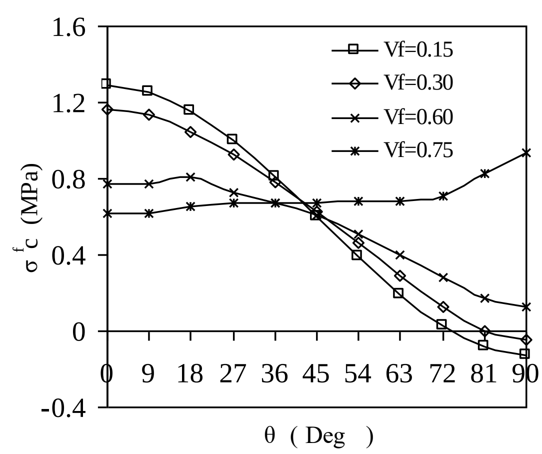

Fig. 10 Variation of bottom interface Circumferential stress in fiber material with respect to θ

Fig. 11 shows the variation of interface circumferential stress in the matrix material with respect to θ. The stresses are observed to be tensile for all the volume fractions. The magnitude of the circumferential stress is observed to be maximum at $\theta = 90^0$ for all volume fractions. The magnitude of the maximum circumferential stress increases with increase in V_f .

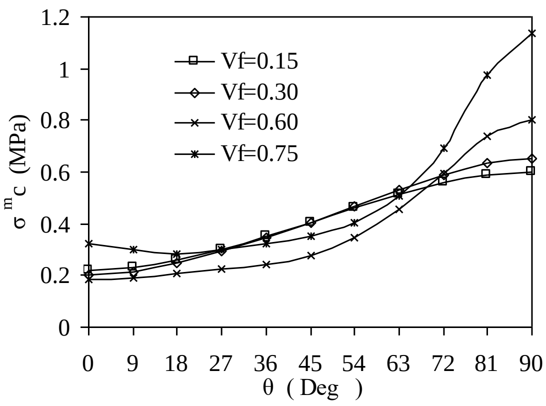

Fig. 11 Variation of bottom interface circumferential stress in matrix material w.r.t. θ

4.2.2 Stresses at top inter face:

Fig. 12 shows the variation of interface normal stress in fiber and matrix with respect to θ. The stresses are observed to be compressive for V_f =15%,30% and 75% up to $\theta = 25^0$ and is tensile in between $\theta = 25^0$ and 90^0. For $V_f = 60\%$ the normal stress is compressive up to $\theta = 9^0$ and is tensile in between 9^0 and 90^0. The magnitude of the stress is observed to be maximum at $\theta = 90^0$. For V_f =15%,30% and 75% it is maximum at $\theta = 0^0$ for $V_f = 60\%$. It is observed that the magnitude of the stress increases up to 60% of V_f and later decreases at $\theta = 0^0$ .For $\theta = 90^0$ the stress increases with increase V_f .

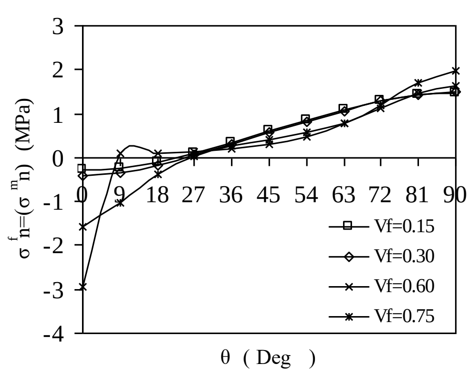

Fig. 12 Variation of top interface Normal stress with respect to θ

The variation of the interface shear stress in both the constituent materials with respect to θ is shown in Fig. 13 .The shear stress is observed to be maximum at $\theta = 45^0$ for volume fractions of 15% and 30%.For V_f = 60% and 75% the stress is maximum at $\theta = 63^0$. It is observed that the magnitude of the maximum shear stress decreases with increase in V_f.

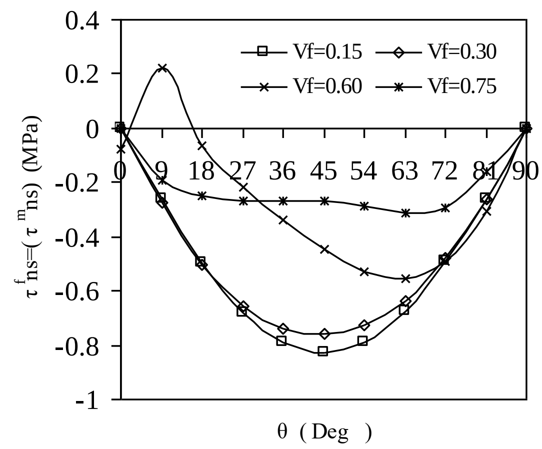

Fig. 13. Variation of top interface Shear stress with respect to θ

Fig.14 shows the variation of interface circumferential stress in the fiber material with respect to θ. The stresses are observed to be tensile for V_f = 15% and 30% up to $\theta = 72^0$ and is compressive in between $\theta = 72^0$ and $\theta = 90^0$ .For V_f = 60% the stress is tensile for all the values of θ. For V_f =75% this stress is compressive up to $\theta = 16^0$ and is tensile in between $\theta = 16^0$ and 90^0 . The magnitude of the circumferential stress is observed to be maximum at $\theta = 0^0$ for volume fractions of 15%, 30% and 60%. For V_f = 75% the stress is maximum at $\theta = 90^0$. It is observed that the stress is maximum at $\theta = 0^0$ for $V_f = 60\%$.

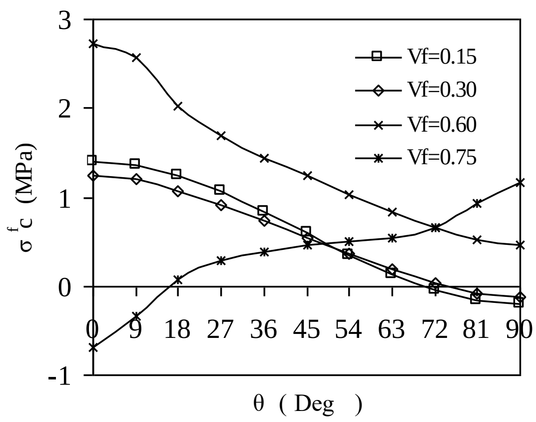

Fig. 14 Variation of top interface circumferential stress in fiber material with respect to θ

Fig. 15 shows the variation of interface circumferential stress in the matrix material with respect to θ. The stress is compressive for V_{f} =15% up to θ = $20^0$and it is tensile in between θ = $20^0$and 90^0 . For V_{f} =30% it is compressive up to θ = 25^0 and is tensile in between θ = $25^0$and 90^0 . . For V_f =60% the stress is compressive up to θ = 8^0 and is tensile in between θ = $8^0$and 90^0 . For V_{f} =75% the stress is compressive up to θ = 16^0 and is tensile in between θ = $16^0$and 90^0 . The magnitude of the circumferential stress is observed to be maximum at θ = 90^0 for V_f = 15%, 30%, and 75% .For V_f =60% it is maximum at θ = 0^0 .The magnitude of the stress increases with increase in V_f at θ = 90^0.

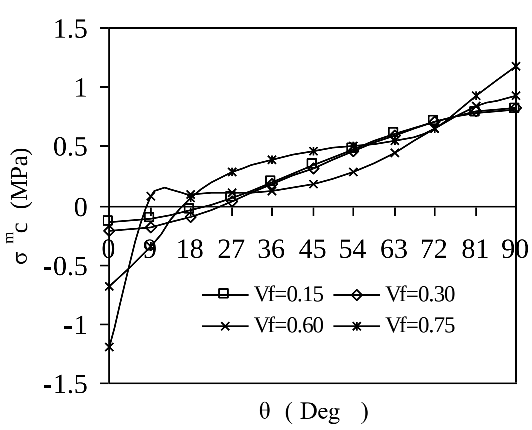

Fig. 15 Variation of top interface circumferential stress in matrix material w.r.t. θ

5. CONCLUSIONS

The micromechanical behavior of hybrid FRP lamina has been studied using finite element method. The Young's modulus E_3 and Poisson's ratios ν_{31} and ν_{32} are predicted for different fiber volume fractions. The stresses at the fiber-matrix interface are also computed. The following conclusions are drawn.

- The Young's modulus is found to be increasing with V_f indicating that the stiffness of the composite increases with V_f .
- The Poisson's Ratios (ν_{32}) decreases with the increase in volume fraction for all the three combinations
- For the top interface, the magnitude of the normal stress at the fiber matrix interface is maximum and tensile at θ = 90^0 for Vf = 15%, 30% and 75% as the direction of the load is normal to the surface at this location. This may result in the separation of fiber and matrix leading to debonding at these locations. **(Figs. 12)**
- The magnitude of the shear stress is observed to be maximum at θ = 45^0 for V_f of 15% and 30% indicating that the interfacial damage may occur at these locations .The shear stress is observed to be maximum at θ = 63^0 and 72^0 for V_f = 60% and 75% respectively indicating that the interfacial damage may occur at these locations at the bottom interface. In unidirectional state of stress the maximum shear stresses will be at an angle of 45^0 to the direction of maximum normal stress. The variation from 45^0 in some of the cases may be due to the constrained effect on the unit cell to make the faces of the unit cell remains straight after loading. **(Figs. 9&13).**
- The magnitude of circumferential stresses in the fiber material are observed to be maximum at θ = 0^0 for V_f = 15%, 30% and 60% this indicates that the failure of fiber occurs at θ = 0^0 at top and bottom interfaces. For V_f = 75% the stress is observed to be maximum at θ = 90^0. This may result in the failure of the fiber at this location at the top and bottom interfaces. **(Figs. 10& 14)**. The maximum circumferential stress at 0^0 location is because the fiber at 0^0 locations is subjected to maximum expansion for V_f up to 60%. At 90^0, this stress in the fiber is compressive due to the compression action of the matrix at lower V_f. As the volume fraction increases, the effect due the matrix decreases and the stress is changing from compression to tensile.
- The magnitude of circumferential stresses in the matrix material are observed to be maximum at θ = 90^0 for all V_f at bottom interface. This indicates that the failure of matrix occurs at θ = 90^0 at bottom interface.

(Figs. 11). The reason for the above effect is at 90^0 location the fiber tries to expand the matrix and this effect increases with increase in the volume fraction.

REFERENCES

1. Chen CH and Cheng S. (1970), "Mechanical properties of anisotropic Fiber-reinforced Composites", Trans. ASME Journal of Applied Mechanics, 37, pp. 186-189.
2. Hashin Z and Rosen BW. (1964), "The elastic moduli of fiber reinforced materials", Trans. ASME Journal of Applied Mechanics, 31, pp. 223-232.
3. Hashin Z. (1965), "On elastic behavior of fiber-reinforced materials of arbitrary transverse phase geometry", Journal of the mechanics and physics of solids, 13, pp. 119-134.
4. Whitney JM. (1967), "Elastic moduli of unidirectional composites with anisotropic filaments", Journal of Composite Materials, 1, pp.188-193.
5. Takashi Ishiwaka, Koyama K and Kobayashi S. (1977), "Elastic moduli of carbon-epoxy composites and carbon fibers", Journal of Composite Materials, 11, pp. 332-344.
6. Hashin Z. (1983), "Analysis of composite materials – A survey. Trans. ASME Journal of Applied Mechanics, 50, pp. 481-505.
7. Hyer MW. (1998), "Stress Analysis of Fiber-Reinforced Composite Materials", Mc. GRAW- HILL International edition.
8. Mohana Rao K. (1986), "Work Shop on Introduction to Fiber-Reinforced Composites", NSTL.
9. Morais AB. (2000), "Transverse moduli of continuous-fiber-reinforced polymers", Composites Science and Technology, 60, pp. 997-1002.
10. Anifantis NK. (2000), "Micromechanical stress analysis of closely packed fibrous composites", Composites Science and Technology, 60, pp. 1241-1248.
11. Sun CT and Vaidya RS. (1996), "Prediction of composite properties from a representative volume element", Composites Science and Technology, 56, pp. 171-179.
12. Li. S. (2000), "General unit cells for micromechanical analyses of unidirectional composites", Composites: part A, 32, pp. 815-826.
13. Yiping Qiu and Peter Schwartz (1993), "Micromechanical behaviour of Kevlar 149/S-Glass hybrid seven fiber microcomposites: I. Tensile strength of the hybrid composite", Composites Science and Technology, 47, pp. 289-301.
14. Mishra and Mohanty (2003), "Studies of mechanical performance of biofiber/glass reinforced polyester hybrid composites", Composites Science and Technology, 63, pp.1377-1385.
15. ANSYS Reference Manuals (2006)
16. Hui-Zushan & Tsu- Wei Chout (1995), "Transverse Elastic Moduli of uni directional Fiber composites with fiber/matrix interfacial de bonding" *Composites Science & Technology*, 53, 383-391